THE EUROPEAN
PHYSICAL JOURNAL C

CrossMark

Regge trajectories for heavy quarkonia from the quadratic form of the spinless Salpeter-type equation

Jiao-Kai Chen[a]

School of Physics and Information Science, Shanxi Normal University, Linfen 041004, China

Abstract In this paper, we present one new form of the Regge trajectories for heavy quarkonia which is obtained from the quadratic form of the spinless Salpeter-type equation (QSSE) by employing the Bohr-Sommerfeld quantization approach. The obtained Regge trajectories take the parameterized form $M^2 = \beta(c_l l + \pi n_r + c_0)^{2/3} + c_1$, which are different from the present Regge trajectories. Then we apply the obtained Regge trajectories to fit the spectra of charmonia and bottomonia. The fitted Regge trajectories are in good agreement with the experimental data and the theoretical predictions.

1 Introduction

The Regge theory [1,2] is based on Lorentz invariance, unitary and analyticity of the scattering matrix and has nothing with quarks and gluons. Due to its generality, the Regge theory is still an indispensable tool in phenomenological studies. The Regge theory is concerned with almost all aspects of strong interactions. One of the most distinctive features of the Regge theory is the Regge trajectory which is one of the effective approaches for studying hadron spectra [3–7].

It is known that the Regge trajectories for the hadrons constituting of light quarks are approximately linear [8–16], that is, the mass M is related to the spin J and the principle quantum number n by

$$M^2 = \alpha J + \beta n + \text{const.}, \tag{1}$$

where α and β are the Regge slopes which are almost equal for light mesons. For heavy mesons, α will be smaller than β [6,17–19]. In Ref. [20], the authors show that the Regge trajectories are nonlinear in case of both fixed and running coupling constants by using the perturbative QCD. In Ref. [21], the authors show by analyzing the data from the UA8

and ISR experiments at CERN that the effective Pomeron Regge trajectories require a term quadratic in t. In Ref. [22], the authors scrutinize the hadronic Regge trajectories in the framework of the string model and the potential model, and recognize that the Regge trajectories for mesons and baryons are not straight and parallel lines in general in the current resonance region both experimentally and theoretically. In Ref. [23], the authors show that meson trajectories are nonlinear and intersecting by fitting experimental data. In Ref. [6], the authors argue that the hadronic Regge trajectories are essentially nonlinear and can be well approximated by a specific square-root form. In Refs. [24,25], the quasilinear Regge trajectories for heavy mesons are discussed. In Refs. [26–28], the authors obtain an interpolating mass formula which gives the nonlinear Regge trajectories.

The idea of nonlinear Regge trajectories is not new [29–35]. Different models and different potentials will effect the Regge trajectories [6,36,37]. Different from the massless string model which produces the linear Regge trajectories, the relativistic string with massive ends will result in the complicated behavior of the Regge trajectories [38–41]. In Ref. [42], the authors obtain the nonlinear Regge trajectories from the gauge/string correspondence. In Ref. [6], the authors present a phenomenological string model for square-root Regge trajectories. In Refs. [43–45], the square-root trajectory is obtained by combining both Regge poles and cuts. The Schrödinger equation with the Cornell potential produces the Regge trajectories $M^2 \sim \beta l^{4/3}$, and the linear Regge trajectories demands the confining potential rising as $r^{2/3}$ [46]. In Ref. [47], the authors show that the Regge trajectories become linear for the Dirac equation with the linear confinement for large orbital angular momenta. The Regge trajectories for the Klein-Gordon equation are considered in Refs. [48–50]. In Ref. [51], the authors obtained the linear, non-intersecting and parallel Regge trajectories by calculating the numerical solutions of the relativistic Thompson equation. In Ref. [52], the authors obtain the nonlinear

[a] e-mails: chenjk@sxnu.edu.cn; chenjkphy@yahoo.com

Regge trajectories by including spin dependent terms in a three-dimensional reduction of the Bethe-Salpeter equation. In case of the spinless Salpeter equation, the Cornell potential or the linear potential can yield linear Regge trajectories [53,54]. In Ref. [55], the authors find straight Regge trajectories in case of light-light quarkonia starting from a first principle Salpeter equation. In Ref. [56], the authors discuss the Regge trajectories by solving the eigenvalue equation with the quadratic mass operator. In this paper, we obtain one new form of the Regge trajectories from the quadratic form of the spinless Salpeter-type equation (QSSE) [57–60] with the Cornell potential or the linear potential. As the obtained new Regge trajectories employed to the spectra of charmonia and bottomonia, the fitted data are in very good agreement with the experimental data and theoretical predictions.

This paper is organized as follows. In Sect. 2, the new form of the Regge trajectories is obtained from the quadratic form of the spinless Salpeter-type equation with the Cornell potential and the power-law potentials. In Sect. 3, the obtained Regge trajectory is applied to fit the spectra of bottomonia and charmonia. We conclude in Sect. 4.

2 Regge trajectories from the quadratic form of the spinless Salpeter-type equation

In this section, we review briefly the QSSE at first. Then we present the orbital and radial Regge trajectory formulas obtained from the QSSE by employing the Bohr-Sommerfeld quantization approach [5,61], which are different from the known Regge trajectories.

2.1 QSSE

The Bethe-Salpeter equation [62,63] is based on the relativistic field theory and is an appropriate tool to deal with bound states. In Ref. [64], a first principal Bethe-Salpeter equation is obtained by using the only assumption that ln W (W being the Wilson loop correlator) can be written in QCD as the sum of its perturbative expression and an area term. By means of a three dimensional reduction, the Bethe-Salpeter equation becomes the eigenvalue equation for the square mass operator [56–58,64,65]

$$M^2 = M_0^2 + U, \qquad (2)$$

where

$$M_0 = \omega_1 + \omega_2 = \sqrt{m_1^2 + \mathbf{p}^2} + \sqrt{m_2^2 + \mathbf{p}^2},$$

$$\langle \mathbf{p}|U|\mathbf{p}'\rangle = \frac{1}{(2\pi)^3}\sqrt{\frac{w_1 + w_2}{2w_1 w_2}}\,\hat{I}_{ab}^{\mathrm{inst}}(\mathbf{p}, \mathbf{p}')\sqrt{\frac{w_1' + w_2'}{2w_1' w_2'}}\,\sigma_1^a \sigma_2^b. \qquad (3)$$
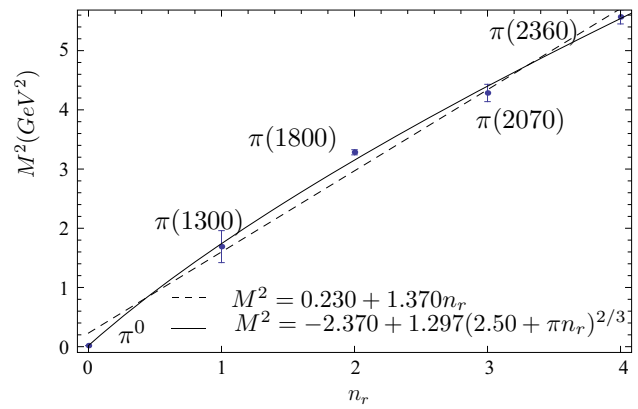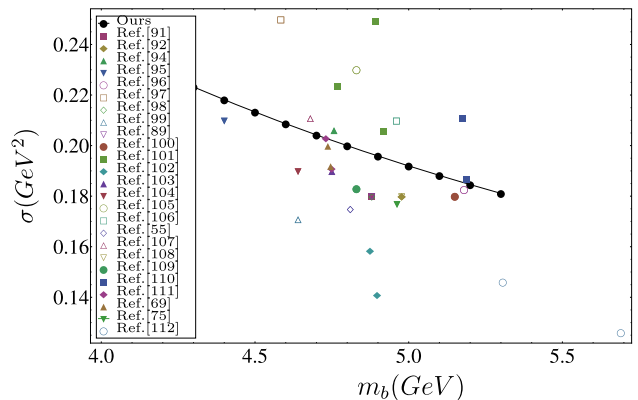

Fig. 1 The radial Regge trajectory of π

Fig. 2 Choice of parameters for various models incorporating the linear potential or the screened linear potential. The joined black line (Ours) is for $\sigma = \beta^{3/2}/(12m_b)$ ($\beta = 5.1$ GeV^2) which is from Eq. (24). σ is the string tension, m_b is the mass of the bottom quark

In the above equations, M is the bound state mass, $\mathbf{p}$ the c.m. momentum of quarks, m_1 and m_2 their constituent masses, $\omega_1' = \sqrt{m_1^2 + \mathbf{p}'^2}$ and $\omega_2' = \sqrt{m_2^2 + \mathbf{p}'^2}$. $\hat{I}_{ab}^{\mathrm{inst}}(\mathbf{p}, \mathbf{p}')$ is the instantaneous kernel. Neglecting any reference to the spin degrees of freedom of the involved bound-state constituents, Eq. (2) reduces to the quadratic form of the spinless Salpeter-type equation which is written in configuration space as [52, 57–60]

$$M^2 \Psi(\mathbf{r}) = [\omega_1 + \omega_2]^2 \Psi(\mathbf{r}) + \mathcal{U}\Psi(\mathbf{r}), \qquad (4)$$

where ω_i is the square-root operator of the relativistic kinetic energy of constituent

$$\omega_i = \sqrt{m_i^2 - \Delta}. \qquad (5)$$

m_i are effective masses in the phenomenological model. The relativistic corrections with $\mathcal{U}$ are small for heavy constituents and will make calculations complicated. Just like the case of the spinless Salpeter equation [66–70], we assume
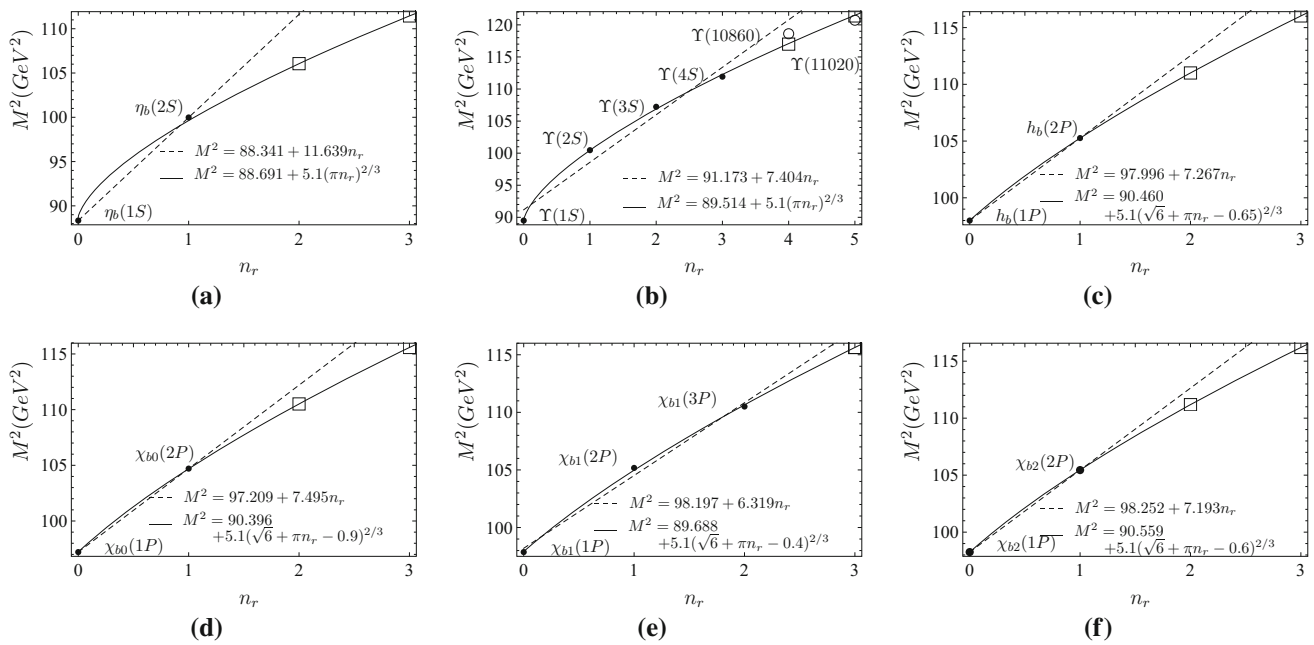
Fig. 3 Radial Regge trajectories for bottomonia. Open squares are predicted masses by the fitted Regge trajectories. The well-established states are given by solid dots and the unsigned states are given by circles
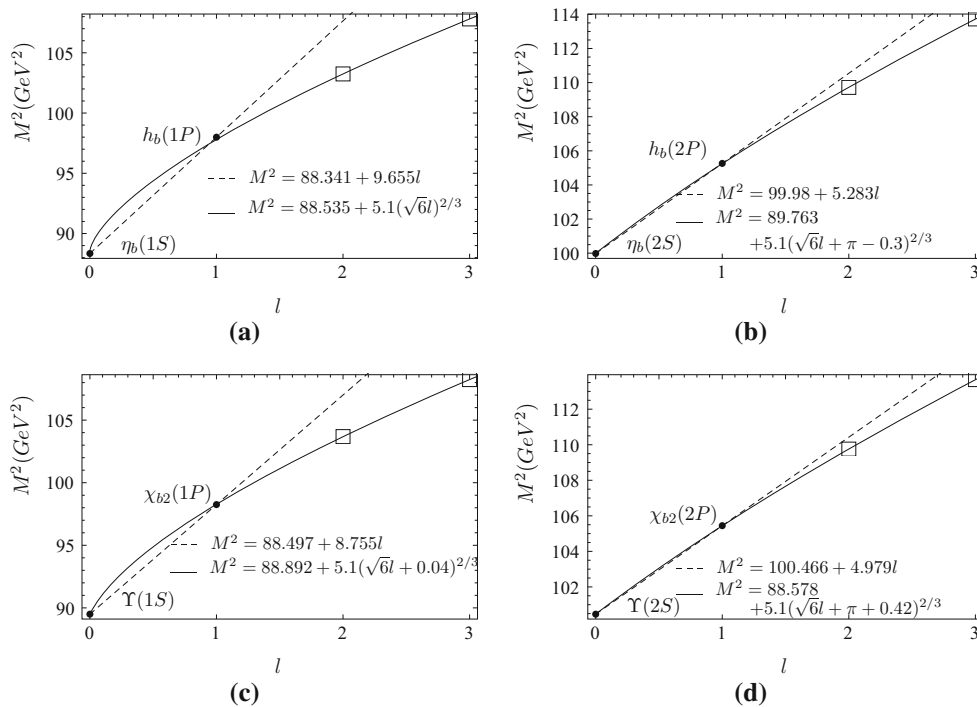

Fig. 4 Same as Fig. 3 except for the orbital Regge trajectories

that $\mathcal{U}$ in Eq. (4) can be taken to be nonrelativistic for simplicity although the kinetic energies of the constituents are taken to be relativistic. In the nonrelativistic limit, the configuration-space $\mathcal{U}$ reduces to

$$\mathcal{U} = 2(m_1 + m_2)V(r), \tag{6}$$

where $V(r)$ is the usual nonrelativistic potential. In this paper, the Cornell potential [71,72] and the power-law potentials are considered,

$$V(r) = -\frac{\alpha}{r} + \sigma r, \quad \sigma r^a. \tag{7}$$

Table 1 Bottomonium masses (in units of MeV) fitted by the radial Regge trajectories [Eq. (26)]. The experimental masses are from PDF [90]. The fitted results by using the Regge trajectories [Eq. (26)] are shown in comparison with the theoretical values of EFG13 [91], GM15 [92], SOEF16 [93] and DLGZ17 [94]. ? denotes the possible candidates for the unwell-established states

State	Meson	J^{PC}	PDG [90]	Fitted	EFG13 [91]	GM15 [92]	SOEF16 [93]	DLGZ17 [94]
1^1S_0	$\eta_b(1S)$	0^{-+}	9399.0 ± 2.3	9418	9398	9402	9455	9390
2^1S_0	$\eta_b(2S)$	0^{-+}	$9999.0 \pm 3.5^{+2.8}_{-1.9}$	9982	9990	9976	9990	9990
3^1S_0	$\eta_b(3S)$	0^{-+}		10,298	10,329	10,336	10,330	10,326
4^1S_0	$\eta_b(4S)$	0^{-+}		10,557	10,573	10,623		10,584
5^1S_0	$\eta_b(5S)$	0^{-+}		10,782	10,851	10,869		10,800
6^1S_0	$\eta_b(6S)$	0^{-+}		10,985	11,061	11,097		10,988
1^3S_1	$\Upsilon(1S)$	1^{--}	9460.30 ± 0.26	9461	9460	9465	9502	9460
2^3S_1	$\Upsilon(2S)$	1^{--}	10023.26 ± 0.31	10,023	10,023	10,003	10,015	10,015
3^3S_1	$\Upsilon(3S)$	1^{--}	10355.2 ± 0.5	10,338	10,355	10,354	10,349	10,343
4^3S_1	$\Upsilon(4S)$	1^{--}	10579.4 ± 1.2	10,596	10,586	10,635	10,607	10,579
5^3S_1	$\Upsilon(10860)?$	1^{--}	$10891.1 \pm 3.2^{+1.2}_{-2.0}$	10,820	10,869	10,878	10,818	10811
6^3S_1	$\Upsilon(11020)?$	1^{--}	$10987.5^{+6.4+9.1}_{-2.5-2.3}$	11,023	11,088	11,102	10,995	10,997
1^1P_1	$h_b(1P)$	1^{+-}	9899.3 ± 0.8	9900	9900	9882	9879	9909
2^1P_1	$h_b(2P)$	1^{+-}	$10259.8 \pm 0.5 \pm 1.1$	10,259	10,260	10,250	10,240	10,254
3^1P_1	$h_b(3P)$	1^{+-}		10,536	10,544	10,541	10,516	10,519
4^1P_1	$h_b(4P)$	1^{+-}		10,772	10,804	10,790		
5^1P_1	$h_b(5P)$	1^{+-}		10,982		11,016		
1^3P_0	$\chi_{b0}(1P)$	0^{++}	$9859.44 \pm 0.42 \pm 0.31$	9860	9859	9847	9855	9864
2^3P_0	$\chi_{b0}(2P)$	0^{++}	$10232.5 \pm 0.4 \pm 0.5$	10,232	10,233	10,226	10,221	10,220
3^3P_0	$\chi_{b0}(3P)$	0^{++}		10,512	10,521	10,522	10,500	10,490
4^3P_0	$\chi_{b0}(4P)$	0^{++}		10,751	10,781	10,775		
5^3P_0	$\chi_{b0}(5P)$	0^{++}		10,963		11,004		
1^3P_1	$\chi_{b1}(1P)$	1^{++}	$9892.78 \pm 0.26 \pm 0.31$	9895	9892	9876	9874	9903
2^3P_1	$\chi_{b1}(2P)$	1^{++}	$10255.46 \pm 0.22 \pm 0.50$	10,246	10,255	10,246	10,236	10,249
3^3P_1	$\chi_{b1}(3P)$	1^{++}	$10512.1 \pm 2.1 \pm 0.9$	10,519	10,541	10,538	10,513	10,515
4^3P_1	$\chi_{b1}(4P)$	1^{++}		10,753	10,802	10,788		
5^3P_1	$\chi_{b1}(5P)$	1^{++}		10,963		11,014		
1^3P_2	$\chi_{b2}(1P)$	2^{++}	$9912.21 \pm 0.26 \pm 0.31$	9912	9912	9897	9886	9921
2^3P_2	$\chi_{b2}(2P)$	2^{++}	$10268.65 \pm 0.22 \pm 0.50$	10,269	10,268	10,261	10,246	10,264
3^3P_2	$\chi_{b2}(3P)$	2^{++}		10,544	10,550	10,550	10,521	10,528
4^3P_2	$\chi_{b2}(4P)$	2^{++}		10,780	10,812	10,798	10,744	
5^3P_2	$\chi_{b2}(5P)$	2^{++}		10,989		11,022		

In Ref. [55], the authors find straight Regge trajectories for the light-light case starting from a first principle Salpeter equation. As a well-defined standard approximation to the Bethe-Salpeter equation, the spinless Salpeter equation [73–75] yields the linear Regge trajectories for the linear potential. In Ref. [56], the Regge trajectories for the light-light quarkonium systems are calculated by using both the linear mass operator and the quadratic mass operator, respectively. The authors notice the differences between two kinds of Regge trajectories. In the following, we will propose one kind of nonlinear Regge trajectories from the QSSE [Eq. (4)] which has a quadratic mass operator.

2.2 Bohr-Sommerfeld quantization approach

In this subsection, we follow Ref. [5] to employ the Bohr-Sommerfeld quantization approach [61] to obtain the orbital Regge trajectories and the radial Regge trajectories from the QSSE.

In case of equally massive constituents ($m_1 = m_2 = m$), the quadratic mass operator of the QSSE with the Cornell potential reads from Eq. (4)

$$M^2 = 4\left(\mathbf{p}^2 + m^2\right) + \mathcal{U}(r), \qquad (8)$$

Table 2 Bottomonium masses (in units of MeV) fitted by the orbital Regge trajectories [Eq. (26)]. The experimental masses are from PDF [90]. The fitted results by using the Regge trajectories [Eq. (26)] are shown in comparison with the theoretical values of EFG13 [91], GM15 [92], SOEF16 [93] and DLGZ17[94]

State	Meson	J^{PC}	PDG [90]	Fitted	EFG13 [91]	GM15 [92]	SOEF16 [93]	DLGZ17 [94]
1^1S_0	$\eta_b(1S)$	0^{-+}	9399.0 ± 2.3	9409	9398	9402	9455	9390
2^1S_0	$\eta_b(2S)$	0^{-+}	$9999.0 \pm 3.5^{+2.8}_{-1.9}$	1000	9990	9976	9990	9990
1^3S_1	$\Upsilon(1S)$	1^{--}	9460.30 ± 0.26	9460	9460	9465	9502	9460
2^3S_1	$\Upsilon(2S)$	1^{--}	10023.26 ± 0.31	10,024	10,023	10,003	10,015	10,015
1^1P_1	$h_b(1P)$	1^{+-}	9899.3 ± 0.8	9890	9900	9882	9879	9909
2^1P_1	$h_b(2P)$	1^{+-}	$10259.8 \pm 0.5 \pm 1.1$	10,259	10,260	10,250	10,240	10,254
1^3P_2	$\chi_{b2}(1P)$	2^{++}	$9912.21 \pm 0.26 \pm 0.31$	9913	9912	9897	9886	9921
2^3P_2	$\chi_{b2}(2P)$	2^{++}	$10268.65 \pm 0.22 \pm 0.50$	10,268	10,268	10,261	10,246	10,264
1^1D_2	$\eta_{b2}(1D)$	2^{-+}		10,161	10,163	10,148	10,123	10,153
2^1D_2	$\eta_{b2}(2D)$	2^{-+}		10,475	10,445	10,450	10,419	10,432
1^3D_3	$\Upsilon_3(1D)$	3^{--}		10,183	10,166	10,155	10,127	10,157
2^3D_3	$\Upsilon_3(2D)$	3^{--}		10,476	10,449	10,455	10,422	10,436
1^1F_3	$h_{b3}(1F)$	3^{+-}		10,383	10,346	10,355	10,322	10,339
2^1F_3	$h_{b3}(2F)$	3^{+-}		10,665	10,614	10,619	10,573	
1^3F_4	$\chi_{b4}(1F)$	4^{++}		10,404	10,349	10,358		10,340
2^3F_4	$\chi_{b4}(2F)$	4^{++}		10,661	10,617	10,622		
1^1G_4	$\eta_{b4}(1G)$	4^{-+}		10,578	10,513	10,530		
2^1G_4	$\eta_{b4}(2G)$	4^{-+}		10,837		10,770		
1^3G_5	$\Upsilon_5(1G)$	5^{--}		10,598		10,532		
2^3G_5	$\Upsilon_5(2G)$	5^{--}		10,830		10,772		

where

$$\mathbf{p}^2 = p_r^2 + \frac{p_\phi^2}{r^2}, \quad \mathcal{U} = 4m\left[-\frac{\alpha}{r} + \sigma r\right]. \tag{9}$$

Due to the central interaction, the orbital angular momentum $p_\phi = L$ is a constant of the motion. From the conservation of the total energy M of the bound state, the radial momentum p_r can be written as

$$p_r = \pm \frac{1}{2r}\sqrt{(M^2 - 4m^2)r^2 - 4L^2 + 4\alpha mr - 4m\sigma r^3}$$
$$= \pm \frac{1}{2r}\sqrt{g(r)}. \tag{10}$$

Solving $g(r) = 0$ gives the three roots of $g(r)$. r_j $(j = 0, 1, 2)$ are

$$r_j = 2\sqrt{\frac{-P}{3}}\cos\left(\frac{\theta + 2\pi j}{3}\right) + \frac{E}{3\sigma}, \tag{11}$$

where

$$E = \frac{M^2 - 4m^2}{4m},$$
$$P = -\frac{1}{3\sigma^2}\left(E^2 + 3\sigma\alpha\right), \quad \cos\theta = -\frac{Q}{2}\sqrt{\frac{27}{-P^3}},$$

$$Q = -\frac{1}{27\sigma^3}\left(2E^3 + 9\sigma\alpha E - 27\frac{\sigma^2}{m}L^2\right). \tag{12}$$

As $r_1 \leq 0 \leq r_2 \leq r_0$, the turning points are $r_- = r_2$ and $r_+ = r_0$. The radial motion takes place between two turning points, r_- and r_+.

The action variables in the Bohr-Sommerfeld quantization approach [61] read

$$J_s = \oint p_s \, dq_s, \tag{13}$$

where s is the degrees of freedom of the bound state, q_s and p_s are the coordinates and conjugate momenta. The integral is performed over one cycle of the motion. The action variables should be quantized,

$$J_s = (n_s + c_s)\, h, \tag{14}$$

where h is the Planck constant, n_s (≥ 0) is an integral quantum number. c_s is a real constant, $c_s = 1/2$ [76]. Using Eqs. (13) and (14) to quantize J_ϕ gives $L = l + c_\phi$, $c_\phi = 1/2$. Quantization of J_r yields

$$m\, r_+ \,(Er_1 + 2\alpha)\, K(\eta) + m\, E\, r_+ \,(r_+ - r_1)\, E(\eta)$$
$$- 3L^2\, \Pi(\pi/2, \gamma, \eta) - \frac{3}{2}\pi\, nr_+\sqrt{r_+ - r_1}\,\sqrt{m\sigma} = 0, \tag{15}$$

where

$$n = n_r + c_r = n_r + \frac{1}{2}, \quad \eta = \frac{r_+ - r_-}{r_+ - r_1}, \quad \gamma = 1 - \frac{r_-}{r_+}. \quad (16)$$

In the above equation, n_r is the radial quantum number. $K(x)$, $E(x)$ and $\Pi(\pi/2, x, y)$ are the complete elliptic integrals of the first, second and third kind, respectively [77].

As angular momenta becomes large, $l \gg n_r$, $r_- \approx r_+$ and $\eta \approx 0$. Then, $\theta = \pi$, $K(\eta) = E(\eta) = \Pi(\pi/2, \gamma, \eta) = \pi/2$. Keeping the leading terms in Eq. (15), the Regge trajectories can be obtained

$$M^2 \sim \beta_l l^{2/3}, \quad \beta_l = 6 \left(2m^2\sigma^2\right)^{1/3}. \quad (17)$$

As the radial quantum number becomes large, i.e., $n_r \gg l$, $r_1 \approx r_- \approx 0$, $\eta \approx 1$. Substituting $r_1 = r_- = 0$ into Eq. (13) yields

$$M^2 \sim \beta_{n_r} n_r^{2/3}, \quad \beta_{n_r} = (12m\pi\sigma)^{2/3}. \quad (18)$$

In case of the power-law potential $V(r) = \sigma r^a$ $(a > 0)$, the orbital Regge trajectories for large l are

$$M^2 \sim \beta_l(a) l^{2a/(a+2)} \quad (l \gg n), \quad (19)$$

where $\beta_l(a)$ reads

$$\beta_l(a) = 4(m\sigma)^{2/(a+2)} \left(1 + \frac{a}{2}\right) \left(\frac{2}{a}\right)^{a/(a+2)}. \quad (20)$$

In Ref. [52], the Regge trajectories similar to Eq. (19) are obtained under the semiclassical limit, however, the authors did not discuss in detail the linear potential case. As n_r becomes large, we have the radial Regge trajectories from Eq. (13)

$$M^2 \sim \beta_{n_r}(a) n_r^{2a/(a+2)} \quad (n_r \gg l). \quad (21)$$

The Regge slope is

$$\beta_{n_r}(a) = 4 (m\sigma)^{2/(a+2)} \left[\frac{a\pi}{B(1/a, 3/2)}\right]^{2a/(a+2)}, \quad (22)$$

where $B(x, y)$ is the beta function [77].

The new form of the Regge trajectories [Eqs. (17) and (18)] are obtained from the QSSE (4) by taking the nonrelativistic approximation (6) and neglecting the spin dependent interactions. If higher corrections are considered, the form of the Regge trajectories will become complicated. Moreover, the employed Bohr-Sommerfeld quantization approach is a semiclassical method and is used as an approximation method. Therefore, the obtained Regge trajectories are
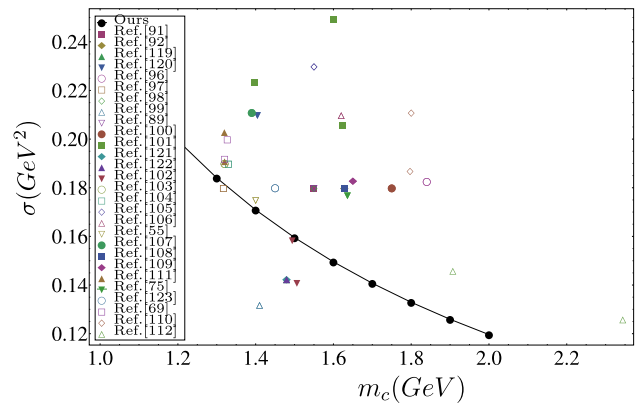

Fig. 5 Choice of parameters for various models incorporating the linear potential or the screened linear potential. The joined black line (Ours) is for $\sigma = \beta^{3/2}/(12m_c)$ ($\beta = 2.02$ GeV^2) which is from Eq. (24). σ is the string tension, m_c is the mass of the charm quark

approximate. For simplicity, we assume the heavy quarkonium Regge trajectories take the simple form. The radial Regge trajectory Eq. (18) can be extended to be of a more general form

$$M^2 = \beta \pi^{2/3} \left(n_r + c'_0\right)^{2/3} + c'_1, \quad (23)$$

where

$$\beta = (12m\sigma)^{2/3}. \quad (24)$$

And the orbital Regge trajectories (17) can be extended to be

$$M^2 = \beta 3^{1/3} \left(l + c''_0\right)^{2/3} + c''_1. \quad (25)$$

By considering Eqs. (23) and (25) and fitting experimental data, we assume that the heavy quarkonium Regge trajectory take the parameterized form

$$M^2 = \beta \left(c_l l + \pi n_r + c_0\right)^{2/3} + c_1. \quad (26)$$

In Eq. (26), β is an universal parameter which has a theoretical value according to Eq. (24). The fitted β for both the bottomonium Regge trajectories and the charmonium Regge trajectories agree well with Eq. (24). c_l is also an universal parameter. The fitted c_l for the bottomonium Regge trajectories ($c_l = \sqrt{6}$) and for the charmonium Regge trajectories ($c_l = \sqrt{5.34}$) deviate from the corresponding theoretical value $c_l = \sqrt{3}$. c_0 and c_1 vary with different trajectories.

The obtained new form of the Regge trajectory [Eq. (26)] is an approximation to the exact unknown one. Out of expectation, by fitting the theoretical values of the Υ ($\Upsilon(1S)$, $\Upsilon(2S)$, $\Upsilon(3S)$, $\Upsilon(4S)$, $\Upsilon(5S)$ and $\Upsilon(6S)$) and ψ ($J/\psi(1S)$, $\psi(2S)$, $\psi(3S)$ and $\psi(4S)$), we find the obtained Regge trajectory [Eq. (26)] is in good agreement with the theoretical values obtained by solving the eigenvalue equation for
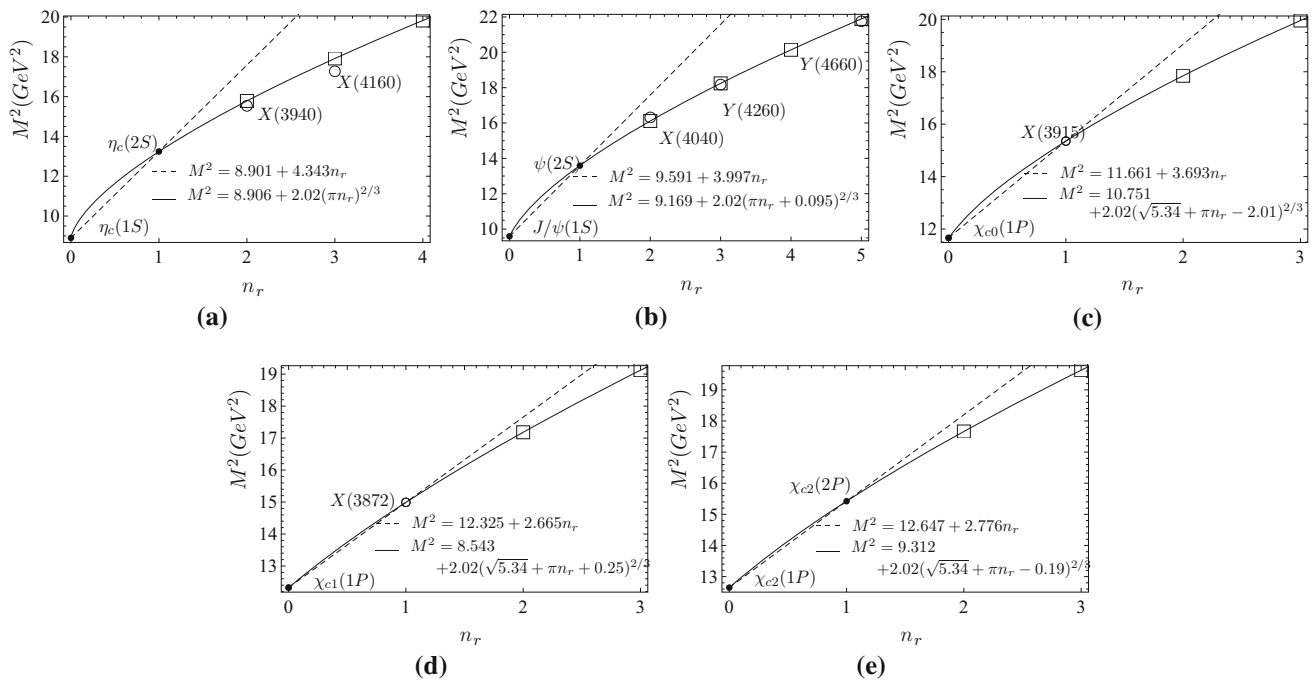
Fig. 6 Radial Regge trajectories for charmonia. The well-established states are given by solid dots and the candidate states are given by circles. Open squares are predicted masses by the fitted Regge trajectories
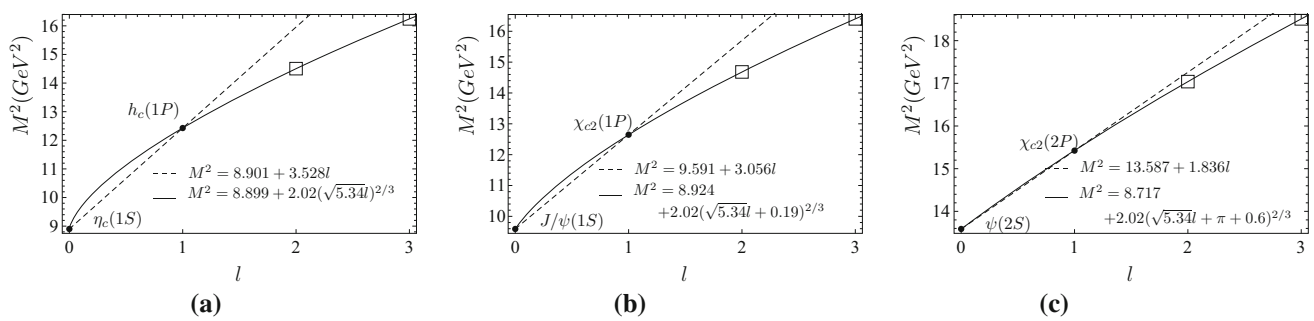

Fig. 7 Same as Fig. 6 except for the orbital Regge trajectories

a squared bound state mass [65]. It suggests that the new Regge trajectories [Eq. (26)] can be applicable not only to QSSE but also to Eq. (2). Moreover, the new form of the Regge trajectories agree well with the experimental data, see Sect. 3.

2.3 Regge trajectories from the Schrödinger equation, the spinless Salpeter equation and the QSSE

There are many discussions on the Regge trajectories in the framework of the Bethe-Salpeter equation and many reductions of it (see the Introduction), however, most of these discussions rely on the numerical solutions and the explicit formula of the Regge trajectories is not given due to the complexity of these equations. In this subsection, we list the explicit formulas of the Regge trajectories for the equations which can be handled easily.

For simplicity, the power-law potentials are considered in this subsection, see Eq. (7). The nonrelativistic Schrödinger equation reads

$$E\psi(\mathbf{r}) = \frac{\mathbf{p}^2}{2\mu}\psi(\mathbf{r}) + \sigma r^a \psi(\mathbf{r}). \qquad (27)$$

The radial and orbital Regge trajectories obtained from Eq. (27) read [5,46], respectively,

$$
\begin{aligned}
M^2 &\sim l^{4a/(a+2)}, &&\text{for large } l, \\
M^2 &\sim n_r^{4a/(a+2)}, &&\text{for large } n_r,
\end{aligned}
\qquad (28)
$$

where $M = m_1 + m_2 + E$. As a relativistic expansion of the Schrödinger equation and a well-defined standard approximation to the Bethe-Salpeter equation, the semirelativistic

spinless Salpeter equation reads

$$M\psi(\mathbf{r}) = \left[\sqrt{\mathbf{p}_1^2 + m_1^2} + \sqrt{\mathbf{p}_2^2 + m_2^2} \right] \psi(\mathbf{r}) + \sigma r^a \psi(\mathbf{r}). \tag{29}$$

The radial and orbital Regge trajectories obtained from Eq. (29) read [5,53,54], respectively,

$$\begin{aligned} M^2 &\sim l^{2a/(a+1)}, &&\text{for large } l, \\ M^2 &\sim n_r^{2a/(a+1)}, &&\text{for large } n_r. \end{aligned} \tag{30}$$

In case of the QSSE, the radial and orbital Regge trajectories read from Eqs. (19) and (21), respectively,

$$\begin{aligned} M^2 &\sim l^{2a/(a+2)}, &&\text{for large } l, \\ M^2 &\sim n_r^{2a/(a+2)}, &&\text{for large } n_r. \end{aligned} \tag{31}$$

For the Schrödinger equation, the linear Regge trajectories need the confining potential rising as $r^{2/3}$; for the spinless Salpeter equation, the linear Regge trajectories demand the linear confining potential; for the QSSE, the linear Regge trajectories need the harmonic-oscillator-type potential.

From Eqs. (28), (30) and (31), we can see that the exponents in the radial and orbital Regge trajectories diminish as the bound-state equations vary from the Schrödinger equation to the spinless Salpeter equation and then to the QSSE. Eqs. (28), (30) and (31) show that different dynamic equations will result in different Regge trajectories although both Eqs. (8) and (29) are reduced from the Bethe-Salpeter equation and the Schrödinger equation can be obtained from Eqs. (8) and (29) by nonrelativistic approximation. The good agreement of the fitted data with the experimental data (see Sect. 3) suggests that the QSSE and the eigenvalue equation for the square mass operator [Eq. (2)] will be better than the Schrödinger equation and the spinless Salpeter equation for heavy quarkonia.

3 Regge trajectories and mass spectra of heavy quarkonia

In this section, we employ the obtained new form of the Regge trajectories to fit the spectra of charmonium and bottomonium. Experimental data are used as inputs to determine the parameters of the Regge trajectories. Then the fitted Regge trajectories can predict the masses of the unobserved states. In this work, the linear Regge trajectories are also fitted by the experimental data and we find that the new form of the Regge trajectories are better than the linear ones.

3.1 Nonlinear Regge trajectories

For light mesons, the Regge trajectories are suggested to be linear although the parameters take different values [78–83]. By fitting the experimental data, we find that the new Regge trajectory is better than the linear one even for π mesons, see Fig. 1 [84]. For heavy quarkonia especially for bottomonia, the Regge trajectories deviate significantly from the linearity. The differences between the results obtained by the linear and the results obtained by the nonlinear Regge trajectories are shown in Figs. 3, 4, 6 and 7.

For the baryon Regge trajectories within the quark-diquark models [85], the radial Regge trajectories for the heavy, light vector mesons [86], the Regge-like relation for the heavy-light systems [87], and the light meson Regge trajectories [8,9,88], the linear confining potential plays dominant role. Similarly, the linear confining potential also dominates the new form of the nonlinear Regge trajectories (26), which can be seen from the derivation in the subsection 2.2. The good fitting of the experimental data by the Regge trajectory (26) confirms this observation and suggests that the contributions of the color Coulomb potential to the heavy quarkonium Regge trajectories is subordinate.

3.2 Masses of Bottomonia

Using the experimental data of the well-established states, the parameters of the radial Regge trajectories, the orbital Regge trajectories and the linear Regge trajectories are determined. Using the masses of pseudoscalar mesons $\eta_b(nS)$ and the masses of the vector mesons $\Upsilon(nS)$, the universal parameter β is calculated, $\beta = 5.1 \text{ GeV}^2$ for bottomonia which is consistent with the theoretical value. According to Eq. (24), there is a relation between the heavy quark mass m and the string tension σ. The chosen value of β for bottomonium is reasonable because the fitted β can be obtained by reasonable m_b and σ, see Fig. 2. (In Fig. 2, the data are from various models with various potentials which incorporating the linear potential or the screened linear potential.)

The universal parameter c_l is calculated by fitting the orbital Regge trajectories for $\eta_b(1S)$ and $\Upsilon(1S)$, $c_l = \sqrt{6}$ for bottomonia. c_0 and c_1 vary with different Regge trajectories. The fitted Regge trajectories are shown in Figs 3 and 4. The fitted and predicted masses of bottomonia by the Regge trajectories are listed in Tables 1 and 2 and they are in good agreement with other theoretical predictions.

The mass of $\Upsilon(10860)$ resonance is $10891.1 \pm 3.2^{+1.2}_{-2.0}$ [90]. $\Upsilon(10860)$ is usually assigned as $\Upsilon(5S)$ [113–116] while it is regarded as one of the strong candidates for the exotic hadron in Ref. [117] due to the unexpectedly large partial widths which disagree with the expectation for a pure $b\bar{b}$ state. The mass of $\Upsilon(11020)$ resonance is $10987.5^{+6.4+9.1}_{-2.5-2.3}$. And $\Upsilon(11020)$ is signed as $\Upsilon(6S)$ [113,114,116]. In Ref.

Table 3 Charmonium masses (in units of MeV) fitted by the radial Regge trajectories [Eq. (26)]. The experimental masses are from PDG [90]. The fitted results by using the Regge trajectories [Eq. (26)] are shown in comparison with the theoretical values of GI85 [131], BGS05 [119], EFG13 [91] and LC09 [120]. ? denotes the possible candidates for the unwell-established states

State	Meson	J^{PC}	PDG [90]	Fitted	GI85 [131]	BGS05 [119]	EFG13 [91]	LC09 [120]
1^1S_0	$\eta_c(1S)$	0^{-+}	2983.4 ± 0.5	2984	2975	2982	2981	2979
2^1S_0	$\eta_c(2S)$	0^{-+}	3639.2 ± 1.2	3639	3623	3630	3635	3623
3^1S_0	$X(3940)?$	0^{-+}	$3942^{+7}_{-6} \pm 6$	3973	4064	4043	3989	3991
4^1S_0	$X(4160)?$	0^{-+}	$4156^{+25}_{-20} \pm 15$	4233	4425	4384	4401	4250
5^1S_0	$\eta_c(5S)$	0^{-+}		4452			4811	4446
6^1S_0	$\eta_c(6S)$	0^{-+}		4645			5155	4595
1^3S_1	$J/\psi(1S)$	1^{--}	3096.900 ± 0.006	3097	3098	3090	3096	3097
2^3S_1	$\psi(2S)$	1^{--}	3686.097 ± 0.010	3686	3676	3672	3685	3673
3^3S_1	$\psi(4040)?$	1^{--}	4039 ± 1	4015	4100	4072	4039	4022
4^3S_1	$Y(4260)?$	1^{--}	4263^{+8}_{-9}	4271	4450	4406	4427	4273
5^3S_1	$\psi(5S)$	1^{--}		4488			4837	4463
6^3S_1	$Y(4660)?$	1^{--}	4664 ± 12	4679			5167	4608
1^3P_0	$\chi_{c0}(1P)$	0^{++}	3414.75 ± 0.31	3414	3445	3424	3413	3433
2^3P_0	$X(3915)?$	0^{++}	3918.4 ± 1.9	3919	3916	3852	3870	3842
3^3P_0	$\chi_{c0}(3P)$	0^{++}		4225	4292	4202	4301	4131
4^3P_0	$\chi_{c0}(4P)$	0^{++}		4467			4698	
1^3P_1	$\chi_{c1}(1P)$	1^{++}	3510.66 ± 0.07	3511	3510	3505	3511	3510
2^3P_1	$X(3872)?$	1^{++}	3871.69 ± 0.17	3872	3953	3925	3906	3901
3^3P_1	$\chi_{c1}(3P)$	1^{++}		4145	4317	4271	4319	4178
4^3P_1	$\chi_{c1}(4P)$	1^{++}		4373			4728	
1^3P_2	$\chi_{c2}(1P)$	2^{++}	3556.20 ± 0.09	3556	3550	3556	3555	3554
2^3P_2	$\chi_{c2}(2P)$	2^{++}	3927.2 ± 2.6	3927	3979	3972	3949	3937
3^3P_2	$\chi_{c2}(3P)$	2^{++}		4203	4337	4317	4354	4208
4^3P_2	$\chi_{c2}(4P)$	2^{++}		4431			4763	

Table 4 Charmonium masses (in units of MeV) fitted by the orbital Regge trajectories [Eq. (26)]. The experimental masses are from PDG [90]. The fitted results by using the Regge trajectories [Eq. (26)] are shown in comparison with the theoretical values of GI85 [131], BGS05 [119], EFG13 [91] and LC09 [120]

State	Meson	J^{PC}	PDG [90]	Fitted	GI85 [131]	BGS05 [119]	EFG13 [91]	LC09 [120]
1^1S_0	$\eta_c(1S)$	0^{-+}	2983.4 ± 0.5	2983	2975	2982	2981	2979
1^3S_1	$J/\psi(1S)$	1^{--}	3096.900 ± 0.006	3097	3098	3090	3096	3097
2^3S_1	$\psi(2S)$	1^{--}	3686.097 ± 0.010	3686	3676	3672	3685	3673
1^1P_1	$h_c(1P)$	1^{+-}	3525.38 ± 0.11	3526	3517	3516	3525	3519
1^3P_2	$\chi_{c2}(1P)$	2^{++}	3556.20 ± 0.09	3556	3550	3556	3555	3554
2^3P_2	$\chi_{c2}(2P)$	2^{++}	3927.2 ± 2.6	3928	3979	3972	3949	3937
1^1D_2	$\eta_{c2}(1D)$	2^{-+}		3808	3837	3799	3807	3796
1^3D_3	$\psi_3(1D)$	3^{--}		3832	3849	3806	3813	3799
2^3D_3	$\psi_3(2D)$	3^{--}		4128	4217	4167	4220	4103
1^1F_3	$h_{c3}(1F)$	3^{+-}		4030	4094	4026	4071	
1^3F_4	$\chi_{c4}(1F)$	4^{++}		4050	4095	4021	4093	
2^3F_4	$\chi_{c4}(2F)$	4^{++}		4302	4425	4348	4434	

[118], the authors propose that $\Upsilon(10580)$, $\Upsilon(10860)$ and $\Upsilon(11020)$ are likely mixtures of conventional $b\bar{b}$ bottomonia and pairs of $B\bar{B}$ or $B_s\bar{B}_s$ mesons.

3.3 Masses of charmonia

The universal parameter β for the radial charmonium Regge trajectories is determined by the masses of pseudoscalar mesons $\eta_c(nS)$ and the masses of the vector mesons $\psi(nS)$, $\beta = 2.02$ GeV^2 for charmonia. According to Eq. (24), the possible values of the charm quark mass m_c and the string tension σ are reasonable, see Fig. 5.

The universal parameter c_l is calculated by fitting the orbital Regge trajectories for $\eta_c(1S)$ and $J/\psi(1S)$, $c_l = \sqrt{5.34}$ for charmonia. c_0 and c_1 vary with different Regge trajectories. The fitted Regge trajectories are in Figs 6 and 7. The fitted and predicted masses of charmonia by the Regge trajectories are listed in Tables 3 and 4 and they are in agreement with other theoretical predictions.

The $X(3940)$ is proposed as the $\eta_c(3S)$ charmonium state [125–128] and $X(4160)$ as the $\eta_c(4S)$ state [129]. In Refs. [119,120,130], the authors argue that the above assignments would imply anomalously large $\Psi(nS) - \eta_c(nS)$ mass splittings .

$X(4040)$ is a hopeful candidate for $\psi(3S)$ [132–135]. $Y(4260)$ is assigned as a normal $c\bar{c}$ state $\psi(4S)$ [136,137]. In Refs. [138,139], the authors argue that $Y(4260)$ is a molecular state. In Refs. [120,121], $Y(4660)$ is taken as a candidate for canonical charmonium state. In Refs. [140,141], $Y(4660)$ is taken as tetraquark state candidate. In Refs. [142,143], $Y(4660)$ is regarded as a $\psi' f_0(980)$ molecule. $Y(4660)$ was also suggested to a baryonium state [144]. The mass of $Y(4660)$ is 4664 ± 12 MeV, which is about equal to the predicted mass [4679 MeV] by the fitted Regge trajectory of charmonium state 6^3S_1, see Fig. 6b and Table 3.

$X(3915)$ is usually identified as the $\chi_{c0}(2p)$ of charmonium based on its mass and likely J^{PC} [130,145] and this assignment has some problems [146].

$X(3872)$ is a candidate for $\chi_{c1}(2P)$ [130]. In Ref. [145], $X(3872)$ is excluded as being the yet-unobserved conventional charmonium state $\chi_{c1}(2P)$. $X(3872)$ is also discussed in the $D^0\bar{D}^{*0}$ hadronic molecular scenario [147].

In Fig 6c and d, masses of $X(3915)$ and $X(3872)$ are used to fit the Regge trajectories. In Fig. 6a, $X(3940)$ and $X(4160)$ lie on the pseudoscalar Regge trajectory. $X(4040)$, $X(4260)$ and $Y(4660)$ lie on the vector Regge trajectory, see Fig. 6b.

4 Conclusions

In this paper, one new form of the Regge trajectories is proposed based on the quadratic form of the spinless Salpeter-type equation and the Bohr-Sommerfeld quantization method. The obtained Regge trajectories for the Cornell potential or for the linear potential take the parameterized form $M^2 = \beta (c_l l + \pi n_r + c_0)^{2/3} + c_1$. The parameters β and c_l and the coefficient π before n_r are universal for bottomonia and charmoniua, respectively. It is shown that the experimental data are very well described by the radial Regge trajectories and the orbital Regge trajectories for both bottomonia and charmonia. The good agreement of the fitted data with the experimental data suggests that the QSSE and the eigenvalue equation for the square mass operator [Eq. (2)] will be good for heavy quarkonia.

One distinctive feature of the new form of the Regge trajectories is that the new form of the heavy quarkonium Regge trajectories and the curvature are determined by the quadratic form of mass operator and the linear potential for long distances which has been validated by lattice QCD calculations, while the contributions of the color Coulomb potential for short distances to the Regge trajectories for heavy quarkonia will be subordinate to that of the linear confining potential.

References

1. T. Regge, Nuovo Cim. **14**, 951 (1959)
2. P.D.B. Collins, Phys. Rept. **1**, 103 (1971)
3. G.F. Chew, S.C. Frautschi, Phys. Rev. Lett. **7**, 394 (1961)
4. G.F. Chew, S.C. Frautschi, Phys. Rev. Lett. **8**, 41 (1962)
5. F. Brau, Phys. Rev. D **62**, 014005 (2000). arXiv:hep-ph/0412170
6. M.M. Brisudova, L. Burakovsky, T. Goldman, Phys. Rev. D **61**, 054013 (2000). arXiv:hep-ph/9906293
7. X.H. Guo, K.W. Wei, X.H. Wu, Phys. Rev. D **78**, 056005 (2008). arXiv:0809.1702 [hep-ph]
8. Y. Nambu, Phys. Rev. D **10**, 4262 (1974)
9. Y. Nambu, Phys. Lett. B **80**, 372 (1979)
10. M. Ademollo, G. Veneziano, S. Weinberg, Phys. Rev. Lett. **22**, 83 (1969)
11. M. Baker, R. Steinke, Phys. Rev. D **65**, 094042 (2002). arXiv:hep-th/0201169
12. J. Polchinski, M.J. Strassler, Phys. Rev. Lett. **88**, 031601 (2002). arXiv:hep-th/0109174
13. A. Karch, E. Katz, D.T. Son, M.A. Stephanov, Phys. Rev. D **74**, 015005 (2006). arXiv:hep-ph/0602229
14. S.J. Brodsky, Eur. Phys. J. A **31**, 638 (2007). arXiv:hep-ph/0610115
15. H. Forkel, M. Beyer, T. Frederico, JHEP **0707**, 077 (2007). arXiv:0705.1857 [hep-ph]
16. S. Filipponi, Y. Srivastava, Phys. Rev. D **58**, 016003 (1998). arXiv:hep-ph/9712204
17. D. Ebert, R.N. Faustov, V.O. Galkin, Eur. Phys. J. C **66**, 197 (2010). arXiv:0910.5612 [hep-ph]

18. D.M. Li, B. Ma, Y.X. Li, Q.K. Yao, H. Yu, Eur. Phys. J. C **37**, 323 (2004). arXiv:hep-ph/0408214
19. A.L. Zhang, Phys. Rev. D **72**, 017902 (2005). arXiv:hep-ph/0408124
20. W.K. Tang, Phys. Rev. D **48**, 2019 (1993). arXiv:hep-ph/9304297
21. A. Brandt et al., UA8 Collaboration. Nucl. Phys. B **514**, 3 (1998). arXiv:hep-ex/9710004
22. A. Inopin, G.S. Sharov, Phys. Rev. D **63**, 054023 (2001). arXiv:hep-ph/9905499
23. A. Tang, J.W. Norbury, Phys. Rev. D **62**, 016006 (2000). arXiv:hep-ph/0004078
24. K.W. Wei, X.H. Guo, Phys. Rev. D **81**, 076005 (2010)
25. L. Burakovsky, L. P. Horwitz, J. T. Goldman, arXiv:hep-ph/9708468
26. M.N. Sergeenko, Phys. Atom. Nucl. **56**, 365 (1993)
27. M .N. Sergeenko, Yad. Fiz **56N3**, 140 (1993)
28. M .N. Sergeenko, Z. Phys. C **64**, 315 (1994)
29. S. Frautschi, B. Margolis, Nuovo Cim. A **56**, 1155 (1968)
30. M. Martinis, Nuovo Cim. A **59**, 490 (1969)
31. H. Yabuki, Phys. Rev. **177**, 2209 (1969)
32. K.V. Vasavada, Phys. Lett. B **34**, 214 (1971)
33. K.V. Vasavada, Phys. Rev. D **3**, 2442 (1971)
34. K.V. Vasavada, Lett. Nuovo Cim. **6**, 453 (1973)
35. V.N. Gribov, E.M. Levin, A.A. Migdal, Sov. J. Nucl. Phys. **12**, 93 (1971)
36. A. E. Inopin, arXiv:hep-ph/0110160, and references therein
37. A.M. Badalian, B.L.G. Bakker, Phys. Rev. D **93**, 074034 (2016). arXiv:1603.04725 [hep-ph]
38. A. Chodos, C.B. Thorn, Nucl. Phys. B **72**, 509 (1974)
39. B.M. Barbashov, V.V. Nesterenko, Theor. Math. Phys. **31**, 465 (1977)
40. I.Y. Kobzarev, L.A. Kondratyuk, B.V. Martemyanov, M.G. Shchepkin, Sov. J. Nucl. Phys. **45**, 330 (1987)
41. I.Y. Kobzarev, B.V. Martemyanov, M.G. Shchepkin, Sov. Phys. Usp. **35**, 257 (1992)
42. L.A. Pando Zayas, J. Sonnenschein, D. Vaman, Nucl. Phys. B **682**, 3 (2004). arXiv:hep-th/0311190
43. K .V. Vasavada, Lett. Nuovo Cim. **6S2**, 453 (1973)
44. K.V. Vasavada, Lett. Nuovo Cim. **6**, 453 (1973)
45. K. V. Vasavada, Print-74-1694 (IUPUI)
46. M. Fabre De La Ripelle, Phys. Lett. B **205**, 97 (1988)
47. M.G. Olsson, S. Veseli, K. Williams, Phys. Rev. D **51**, 5079 (1995). arXiv:hep-ph/9410405
48. J.S. Kang, H.J. Schnitzer, Phys. Rev. D **12**, 841 (1975)
49. L.K. Sharma, V.P. Iyer, J. Math. Phys. **23**, 1185 (1982)
50. D. A. Kulikov, R. S. Tutik, arXiv:hep-ph/0608260
51. D.E. Kahana, K.M. Maung, J.W. Norbury, Phys. Rev. D **48**, 3408 (1993)
52. E. Di Salvo, L. Kondratyuk, P. Saracco, Z. Phys. C **69**, 149 (1995). arXiv:hep-ph/9411309
53. A. Martin, Z. Phys. C **32**, 359 (1986)
54. W. Lucha, F.F. Schöberl, D. Gromes, Phys. Rept. **200**, 127 (1991)
55. M. Baldicchi, G.M. Prosperi, Phys. Lett. B **436**, 145 (1998). arXiv:hep-ph/9803390
56. M. Baldicchi, arXiv: hep-ph/9911268
57. M. Baldicchi, A.V. Nesterenko, G.M. Prosperi, D.V. Shirkov, C. Simolo, Phys. Rev. Lett. **99**, 242001 (2007). arXiv:0705.0329 [hep-ph]
58. M. Baldicchi, G.M. Prosperi, Phys. Rev. D **62**, 114024 (2000). arXiv:hep-ph/0008017
59. J.K. Chen, Acta Phys. Pol. B **47**, 1155 (2016)
60. J.K. Chen, Rom. J. Phys. **62**, 119 (2017)
61. S. Tomonaga, *Quantum Mechanics, Volume I: Old Quantum Theory* (North-Holland Publishing Company, Amsterdam, 1962)
62. E.E. Salpeter, H.A. Bethe, Phys. Rev. **84**, 1232 (1951)
63. E.E. Salpeter, Phys. Rev. **87**, 328 (1952)
64. N. Brambilla, E. Montaldi, G.M. Prosperi, Phys. Rev. D **54**, 3506 (1996). arXiv:hep-ph/9504229
65. M. Baldicchi, A.V. Nesterenko, G.M. Prosperi, C. Simolo, Phys. Rev. D **77**, 034013 (2008). arXiv:0705.1695 [hep-ph]
66. B. Durand, L. Durand, Phys. Rev. D **28**, 396 (1983)
67. B. Durand, L. Durand, Phys. Rev. D **50**, 6662(E) (1994)
68. W. Lucha, H. Rupprecht, F.F. Schoberl, Phys. Rev. D **45**, 1233 (1992)
69. S. Jacobs, M.G. Olsson, C. Suchyta III, Phys. Rev. D **33**, 3338 (1986)
70. S. Jacobs, M.G. Olsson, C. Suchyta III, Phys. Rev. D **34**, 3536(E) (1986)
71. E. Eichten, K. Gottfried, T. Kinoshita, J.B. Kogut, K.D. Lane, T.M. Yan, Phys. Rev. Lett. **34**, 369 (1975)
72. E. Eichten, K. Gottfried, T. Kinoshita, J.B. Kogut, K.D. Lane, T.M. Yan, Phys. Rev. Lett. **36**, 1276(E) (1976)
73. D.P. Stanley, D. Robson, Phys. Rev. D **21**, 3180 (1980)
74. W. Lucha, F.F. Schöberl, Fizika B **8**, 193 (1999). arXiv:hep-ph/9812526
75. A. Gara, B. Durand, L. Durand, L.J. Nickisch, Phys. Rev. D **40**, 843 (1989)
76. R.E. Langer, Phys. Rev. **51**, 669 (1937)
77. I.S. Gradshteyn, I.M. Ryzhik, *Table of Integrals, Series, and Products*, corrected and, enlarged edition (Academic Press, New York, 1980)
78. A.V. Anisovich, V.V. Anisovich, A.V. Sarantsev, Phys. Rev. D **62**, 051502 (2000). arXiv:hep-ph/0003113
79. V. V. Anisovich, Phys. Usp. **47**, 45 (2004)
80. V .V. Anisovich, Usp. Fiz. Nauk **47**, 49 (2004). arXiv:hep-ph/0208123
81. D.V. Bugg, Phys. Rept. **397**, 257 (2004). arXiv:hep-ex/0412045
82. S.S. Afonin, Phys. Rev. C **76**, 015202 (2007). arXiv:0707.0824 [hep-ph]
83. D. Ebert, R.N. Faustov, V.O. Galkin, Phys. Rev. D **79**, 114029 (2009). arXiv:0903.5183 [hep-ph]
84. J. K. Chen, in preparation
85. P. Masjuan, E.Ruiz Arriola, Phys. Rev. D **96**(5), 054006 (2017). arXiv:1707.05650 [hep-ph]
86. S .S. Afonin, I .V. Pusenkov, Phys. Rev. D **90**(9), 094020 (2014). arXiv:1411.2390 [hep-ph]
87. K. Chen, Y. Dong, X. Liu, Q .F. Lü, T. Matsuki, Eur. Phys. J. C **78**(1), 20 (2018). arXiv:1709.07196 [hep-ph]
88. R.R. Mendel, H.D. Trottier, Phys. Rev. D **42**, 911 (1990)
89. D. Ebert, R.N. Faustov, V.O. Galkin, Eur. Phys. J. C **71**, 1825 (2011). arXiv:1111.0454 [hep-ph]
90. C. Patrignani *et al.* [Particle Data Group], Chin. Phys. C **40**, no. 10, 100001 (2016)
91. D. Ebert, R. N. Faustov and V. O. Galkin, Conference: C13-07-15.9, 52 (2013)
92. S. Godfrey, K. Moats, Phys. Rev. D **92**(5), 054034 (2015). arXiv:1507.00024 [hep-ph]
93. J. Segovia, P .G. Ortega, D .R. Entem, F. Fernández, Phys. Rev. D **93**(7), 074027 (2016). arXiv:1601.05093 [hep-ph]
94. W .J. Deng, H. Liu, L .C. Gui, X .H. Zhong, Phys. Rev. D **95**(7), 074002 (2017). arXiv:1607.04696 [hep-ph]
95. B.Q. Li, K.T. Chao, Commun. Theor. Phys. **52**, 653 (2009). arXiv:0909.1369 [hep-ph]
96. E.J. Eichten, C. Quigg, Phys. Rev. D **49**, 5845 (1994). arXiv:hep-ph/9402210
97. N.R. Soni, B.R. Joshi, R.P. Shah, H.R. Chauhan, J.N. Pandya. arXiv:1707.07144 [hep-ph]
98. D. Ebert, R.N. Faustov, V.O. Galkin, Phys. Rev. D **67**, 014027 (2003). arXiv:hep-ph/0210381
99. W.W. Repko, M.D. Santia, S.F. Radford, Nucl. Phys. A **924**, 65 (2014). arXiv:1211.6373 [hep-ph]

100. H.M. Choi, C.R. Ji, Z. Li, H.Y. Ryu, Phys. Rev. C **92**(5), 055203 (2015). arXiv:1502.03078 [hep-ph]
101. S. Leitão, A. Stadler, M.T. Peña, E.P. Biernat, Phys. Rev. D **96**(7), 074007 (2017). arXiv:1707.09303 [hep-ph]
102. K. Igi, S. Ono, Phys. Rev. D **33**, 3349 (1986)
103. K. Hagiwara, A.D. Martin, A.W. Peacock, Z. Phys. C **33**, 135 (1986)
104. D.S. Hwang, C.S. Kim, W. Namgung, Phys. Rev. D **53**, 4951 (1996). arXiv:hep-ph/9506476
105. C.H. Chang, J.Y. Cui, J.M. Yang, Commun. Theor. Phys. **39**, 197 (2003). arXiv:hep-ph/0211164
106. Z.H. Wang, G.L. Wang, C.H. Chang, J. Phys. G **39**, 015009 (2012). arXiv:hep-ph/1107.0474 [hep-ph]
107. A. Abd El-Hady, J.R. Spence, J.P. Vary, Phys. Rev. D **71**, 034006 (2005). arXiv:hep-ph/0603139
108. S. Godfrey, Phys. Rev. D **70**, 054017 (2004). arXiv:hep-ph/0406228
109. C.F. Qiao, H.W. Huang, K.T. Chao, Phys. Rev. D **54**, 2273 (1996). arXiv:hep-ph/9603274
110. W. Lucha, H. Rupprecht, F.F. Schoberl, Phys. Rev. D **46**, 1088 (1992)
111. L.P. Fulcher, Phys. Rev. D **50**, 447 (1994)
112. M. Beyer, U. Bohn, M.G. Huber, B.C. Metsch, J. Resag, Z. Phys. C **55**, 307 (1992)
113. A. Abdesselam *et al.* [Belle Collaboration], Phys. Rev. Lett. **117**(14), 142001 (2016). arXiv:1508.06562 [hep-ex]
114. D. Santel *et al.* [Belle Collaboration], Phys. Rev. D **93**(1), 011101 (2016). arXiv:1501.01137 [hep-ex]
115. R. Oncala, J. Soto, Phys. Rev. D **96**(1), 014004 (2017). arXiv:1702.03900 [hep-ph]
116. N. Akbar, M.A. Sultan, B. Masud, F. Akram, Phys. Rev. D **95**(7), 074018 (2017). arXiv:1511.03632 [hep-ph]
117. M. Takizawa [Belle Collaboration], Conference: C16-07-18.8, p.198,
118. A.E. Bondar, R.V. Mizuk, M.B. Voloshin, Mod. Phys. Lett. A **32**(04), 1750025 (2017). arXiv:1610.01102 [hep-ph]
119. T. Barnes, S. Godfrey, E.S. Swanson, Phys. Rev. D **72**, 054026 (2005). arXiv:hep-ph/0505002
120. B.Q. Li, K.T. Chao, Phys. Rev. D **79**, 094004 (2009). arXiv:0903.5506 [hep-ph]
121. G.J. Ding, J.J. Zhu, M.L. Yan, Phys. Rev. D **77**, 014033 (2008). arXiv:0708.3712 [hep-ph]
122. M.A. Sultan, N. Akbar, B. Masud, F. Akram, Phys. Rev. D **90**(5), 054001 (2014). arXiv:1403.6941 [hep-ph]
123. L.J. Nickisch, L. Durand, B. Durand, Phys. Rev. D **30**, 660 (1984)
124. L.J. Nickisch, L. Durand, B. Durand, Phys. Rev. D **30**, 1995(E) (1984)
125. H.X. Chen, W. Chen, X. Liu, S.L. Zhu, Phys. Rept. **639**, 1 (2016). arXiv:1601.02092 [hep-ph]
126. J.L. Rosner, A.I.P. Conf, Proc. **815**, 218 (2006). arXiv:hep-ph/0508155
127. S.S. Gershtein, A.K. Likhoded, A.V. Luchinsky, Phys. Rev. D **74**, 016002 (2006). arXiv:hep-ph/0602048
128. V.V. Braguta, A.K. Likhoded, A.V. Luchinsky, Phys. Rev. D **74**, 094004 (2006). arXiv:hep-ph/0602232
129. K.T. Chao, Phys. Lett. B **661**, 348 (2008). arXiv:0707.3982 [hep-ph]
130. S. L. Olsen, PoS Bormio **050** (2015). arXiv:1511.01589 [hep-ex]
131. S. Godfrey, N. Isgur, Phys. Rev. D **32**, 189 (1985)
132. E. Eichten, S. Godfrey, H. Mahlke, J.L. Rosner, Rev. Mod. Phys. **80**, 1161 (2008). arXiv:hep-ph/0701208
133. M. Ablikim *et al.* [BES Collaboration], eConf C **070805**, 02 (2007)
134. M. Ablikim et al., Phys. Lett. B **660**, 315 (2008). arXiv:0705.4500 [hep-ex]
135. L.P. He, D.Y. Chen, X. Liu, T. Matsuki, Eur. Phys. J. C **74**(12), 3208 (2014). arXiv:1405.3831 [hep-ph]
136. F.J. Llanes-Estrada, Phys. Rev. D **72**, 031503 (2005). arXiv:hep-ph/0507035
137. M. Shah, K. Thakkar, A. Parmar and P.C. Vinodkumar, arXiv:1312.7664 [hep-ph]
138. Y. Lu, M.N. Anwar, B.S. Zou, Phys. Rev. D **96**, 114022 (2017). arXiv:1705.00449 [hep-ph]
139. B. Durkaya, M. Bayar, EPJ Web Conf. **137**, 06003 (2017)
140. Z.G. Wang, Eur. Phys. J. C **76**(7), 387 (2016). arXiv:1601.05541 [hep-ph]
141. M. Nielsen, F.S. Navarra, S.H. Lee, Phys. Rept. **497**, 41 (2010). arXiv:0911.1958 [hep-ph]
142. F.K. Guo, C. Hanhart, U.G. Meissner, Phys. Lett. B **665**, 26 (2008). arXiv:0803.1392 [hep-ph]
143. P. Hagen, H.-W. Hammer, C. Hanhart, Phys. Lett. B **696**, 103 (2011). arXiv:1007.1126 [hep-ph]
144. C.F. Qiao, J. Phys. G **35**, 075008 (2008). arXiv:0709.4066 [hep-ph]
145. R.F. Lebed, R.E. Mitchell, E.S. Swanson, Prog. Part. Nucl. Phys. **93**, 143 (2017). arXiv:1610.04528 [hep-ph]
146. S.L. Olsen, Phys. Rev. D **91**(5), 057501 (2015). arXiv:1410.6534 [hep-ex]
147. F.K. Guo, C. Hanhart, U.G. Meißner, Q. Wang, Q. Zhao, B.S. Zou, arXiv:1705.00141 [hep-ph]